

## Horizontal variability 1–2 km below the tropical tropopause

A. F. Tuck,<sup>1</sup> S. J. Hovde,<sup>1,2</sup> K. K. Kelly,<sup>1</sup> S. J. Reid,<sup>1,2,3</sup> E. C. Richard,<sup>1,2</sup> E. L. Atlas,<sup>4</sup> S. G. Donnelly,<sup>4</sup> V. R. Stroud,<sup>4</sup> D. J. Cziczo,<sup>1,2</sup> D. M. Murphy,<sup>1</sup> D. S. Thomson,<sup>1,2</sup> J. W. Elkins,<sup>5</sup> F. L. Moore,<sup>2,5</sup> E. A. Ray,<sup>1,2,5</sup> M. J. Mahoney,<sup>6</sup> and R. R. Friedl<sup>6</sup>

Received 2 July 2003; revised 16 December 2003; accepted 31 December 2003; published 13 March 2004.

[1] Two long meridional flights of the WB57F high-altitude aircraft 1–2 km below the tropical tropopause are examined for ozone and total water variability in the context of a large suite of tracers having lifetimes ranging from  $10^{-2}$  to  $10^3$  years, together with mass spectra of individual aerosol particles. It is concluded that local correlations are predominant; contributing processes to the maintenance of the composition are marine convection, continental convection, in situ chemical production, biomass burning, downward transport from the stratosphere and recirculation. *INDEX TERMS:* 0315

Atmospheric Composition and Structure: Biosphere/atmosphere interactions; 0365 Atmospheric Composition and Structure: Troposphere—composition and chemistry; 0368 Atmospheric Composition and Structure: Troposphere—constituent transport and chemistry; 3362 Meteorology and Atmospheric Dynamics: Stratosphere/troposphere interactions; 3374 Meteorology and Atmospheric Dynamics: Tropical meteorology;

*KEYWORDS:* tropical, troposphere, composition

**Citation:** Tuck, A. F., et al. (2004), Horizontal variability 1–2 km below the tropical tropopause, *J. Geophys. Res.*, 109, D05310, doi:10.1029/2003JD003942.

### 1. Introduction

[2] There has been renewed interest in the ozone, water and tracer content of the upper tropical troposphere since the first simultaneous high-altitude aircraft profiles were obtained there by the ER-2 in 1987 and 1994 [Kelly *et al.*, 1993; Tuck *et al.*, 1997]. Folkins *et al.* [1999] analyzed ozonesondes and aircraft data to confirm earlier ideas that much tropical convection did not penetrate beyond 14 km altitude [Murgatroyd, 1965; Ludlam, 1980], and there have been attempts at modeling upper tropospheric humidity [Dessler and Sherwood, 2000; Gettelman *et al.*, 2000; Jensen *et al.*, 2001]. Satellite analyses of humidity in the upper troposphere and lower stratosphere have been performed [Sassi *et al.*, 2001; Clark *et al.*, 2001]. The composition of the upper tropical troposphere (UTT) is important for both climatic reasons and because it forms the chemical feedstock in air entering the photochemically dominated stratosphere above. A general schematic is shown in Figure 1. It should be noted that the tropopause is rarely a continuous surface locally near the subtropical jet streams and actu-

ally slopes upward and poleward between the inner tropics and the jet core in potential temperature coordinates, see, e.g., Tuck *et al.* [2003].

[3] Vertical profiles of tracers through the tropical tropopause justify the notion of a tropical tropopause layer, because there is evidence of a fraction of recently stratospheric air below the tropopause [Tuck *et al.*, 1997]. Immediately above the tropopause, air undepleted in tropospheric tracers is not usually seen; this result implies horizontal transport of “older” stratospheric air from higher latitudes [Volk *et al.*, 1996; Tuck *et al.*, 1997; Herman *et al.*, 1998; Flocke *et al.*, 1999]. However, the traditionally defined tropopause is well-delineated in the tropics for the vast majority of radiosonde ascents and aircraft profiles; the frequency of occurrence of a sharp thermal tropopause is higher than it is in midlatitudes [Bethan *et al.*, 1996], for example.

[4] There are no published horizontal observations of water, ozone and tracers in the upper tropical troposphere, the region below 90 and above 200 hPa between the subtropical jet streams. Some recent analysis of this region has worked in terms of single-valued ozone and water vertical profiles, often interpreted in terms of gross, large-scale dynamics. It will be seen that such grossly average constructs have little or no explanatory power in the context of observed molecular distributions, implying that the transport demands explicit treatment of all scales of motion: simple concepts like “ascent in the Intertropical Convergence Zone (ITCZ), descent in the subtropics” are of little value. Here we use two flights which were planned to examine the horizontal variability of air just below the tropical tropopause.

[5] During the Atmospheric Chemistry of Combustion Emissions Near the Tropopause (ACCENT) mission in

<sup>1</sup>NOAA Aeronomy Laboratory, Boulder, Colorado, USA.

<sup>2</sup>Also at Cooperative Institute for Research in Environmental Sciences, University of Colorado, Boulder, Colorado, USA.

<sup>3</sup>Climate Dynamics Program, National Science Foundation, Washington, DC, USA.

<sup>4</sup>Atmospheric Chemistry Division, NCAR, Boulder, Colorado, USA.

<sup>5</sup>NOAA Climate Monitoring and Diagnostics Laboratory, Boulder, Colorado, USA.

<sup>6</sup>Jet Propulsion Laboratory, California Institute of Technology, Pasadena, California, USA.

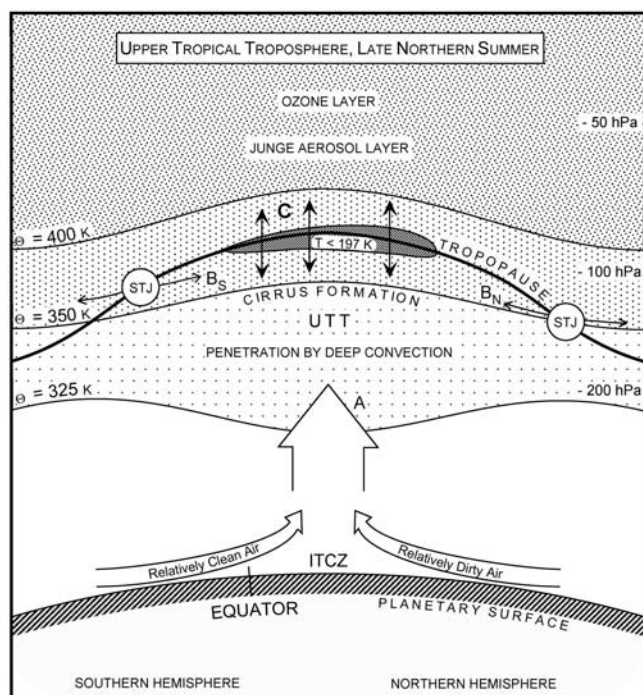


**Figure 1.** A general schematic of processes affecting the composition of the upper tropical troposphere (UTT). Note that the Intertropical Convergence Zone (ITCZ) is shown north of the geographical equator during northern summer and autumn. Evidence for the flow processes labeled A, B<sub>N</sub>, and C is discussed.

1999, the WB57F aircraft completed two long legs 1–2 km below the tropical tropopause, from (29°N, 95°W) to (5°N, 95°W) on 19990920, and from (10°N, 86°W) to (29°N, 95°W) on 19990921 (dates are in yyyyymmdd format). It was equipped with a comprehensive payload for examining chemistry, aerosols and dynamics, and flew at a nominal altitude of 50,000 feet ( $\theta \approx 360$  K,  $P \approx 125$  mb,  $z \approx 15$  km), with the intent of establishing the composition of air about to enter the stratosphere. Few aircraft can cruise at this altitude. Note, however, that there was no explicit study of ice crystals in cirrus; what has been recorded is the occurrence of supersaturation with respect to ice in the total water measurement. The Microwave Temperature Profiler (MTP) [Denning *et al.*, 1989] showed that the tropical thermal tropopause was well-defined and  $\sim 1$ –2 km above the aircraft on both days, see Figures 2b and 3b.

[6] These two flights comprise a new set of detailed tracer and chemical observations in the upper tropical troposphere, and here we analyze the data, drawing conclusions about the maintenance of the composition of the UTT in the Central American region in late September.

## 2. Methods

[7] The WB57F aircraft is capable of horizontal legs at altitudes of 45,000 to 62,000 feet up to 40° great circle degrees (4500 km) in length. On the flights of interest here, the payload included instruments for measuring ozone [Proffitt *et al.*, 1989], total water [Kelly *et al.*, 1989], methane [Richard *et al.*, 2002] at high frequency (0.5 to

1 Hz) and the lower frequency measurements of N<sub>2</sub>O, CH<sub>4</sub>, CO, CCl<sub>2</sub>F<sub>2</sub>, CCl<sub>3</sub>F and SF<sub>6</sub> made by electron capture gas chromatography with the Lightweight Airborne Chromatograph Experiment (LACE) [Moore *et al.*, 2003], and of many species by the whole air sampling (WAS) method [Flocke *et al.*, 1999; Schauffler *et al.*, 1999]. Among the whole air species we consider CH<sub>3</sub>I and CH<sub>3</sub>Cl, together with C<sub>2</sub>H<sub>6</sub>, i-butane and n-pentane. The chemical content of aerosols, from individual particle mass spectra [Murphy *et al.*, 1998], is also used. We note that more comprehensive analysis of the wide suite of non-methane hydrocarbons and halocarbons measured by WAS is in progress [Ridley *et al.*, 2004].

[8] Satellite images were taken from the mission archive, and are GOES-8 infrared pictures with cloud top temperatures colder than  $-35^{\circ}\text{C}$  highlighted at  $10^{\circ}\text{C}$  intervals. Back trajectories were calculated for 5 days, in three dimensions, at  $1^{\circ}$  latitude intervals along both flight tracks, using ECMWF assimilations on 50 levels at  $1^{\circ} \times 1^{\circ}$  latitude - longitude spacing.

## 3. Results

[9] The GOES-8 infrared picture for 19990920 is shown in Figure 2a, with the flight track at  $\sim 125$  mb pressure ( $\theta \approx 360$  K) marked. The climb out from Ellington Field (30°N, 95°W) and the stratospheric segment of the flight (5°N, 87°W) to (10°N, 86°W), which preceded descent to San Jose, Costa Rica (10°N, 86°W), are not shown in Figures 2–6 but are in Figures 7–13. In Figure 3, the equivalent information is given for the upper troposphere flight track segment from (11°N, 80°W) to (29°N, 95°W) on 19990921.

### 3.1. Ozone and Total Water

[10] Perhaps the first thing to note is the range, variation and correlation between ozone and total water. On 19990920, the ozone ranges between 20 and 129 ppbv, with total water ranging from 6 ppmv to 17 ppmv (Figure a); the scatterplot shows at least 4 major populations (Figure 4b). The same information for 19990921 is shown in Figure 5; the ozone ranges from 3 to 122 ppbv, while total water ranges between 4 and 16 ppmv (Figure 5a). There are as many as 6 different major populations on the scatterplot (Figure 5b). There is no simple correlation between ozone and total water in the upper tropical troposphere during these flights, except perhaps poleward of 25°N. On 19990920, there was a tendency for a population having a roughly constant ozone abundance with variable total water at the higher latitudes, together with two populations at the lower latitudes having the reverse characteristics. However, there was considerable physical overlap in these three populations (Figure 4b). The situation was even more complicated on the following day (Figure 5b).

[11] In order to address the meaning of correlation plots in the UTT, we display scattergrams of ozone against methyl iodide (Figure 6a), carbon monoxide (Figure 6b), methane (Figure 6c), nitrous oxide (Figure 6d) and sulfur hexafluoride (Figure 6e) for 19990920. The respective orders of magnitude of the atmospheric lifetimes of these species are  $10^{-2}$ ,  $10^{-1}$ , 10,  $10^2$  and  $10^3$  years respectively.



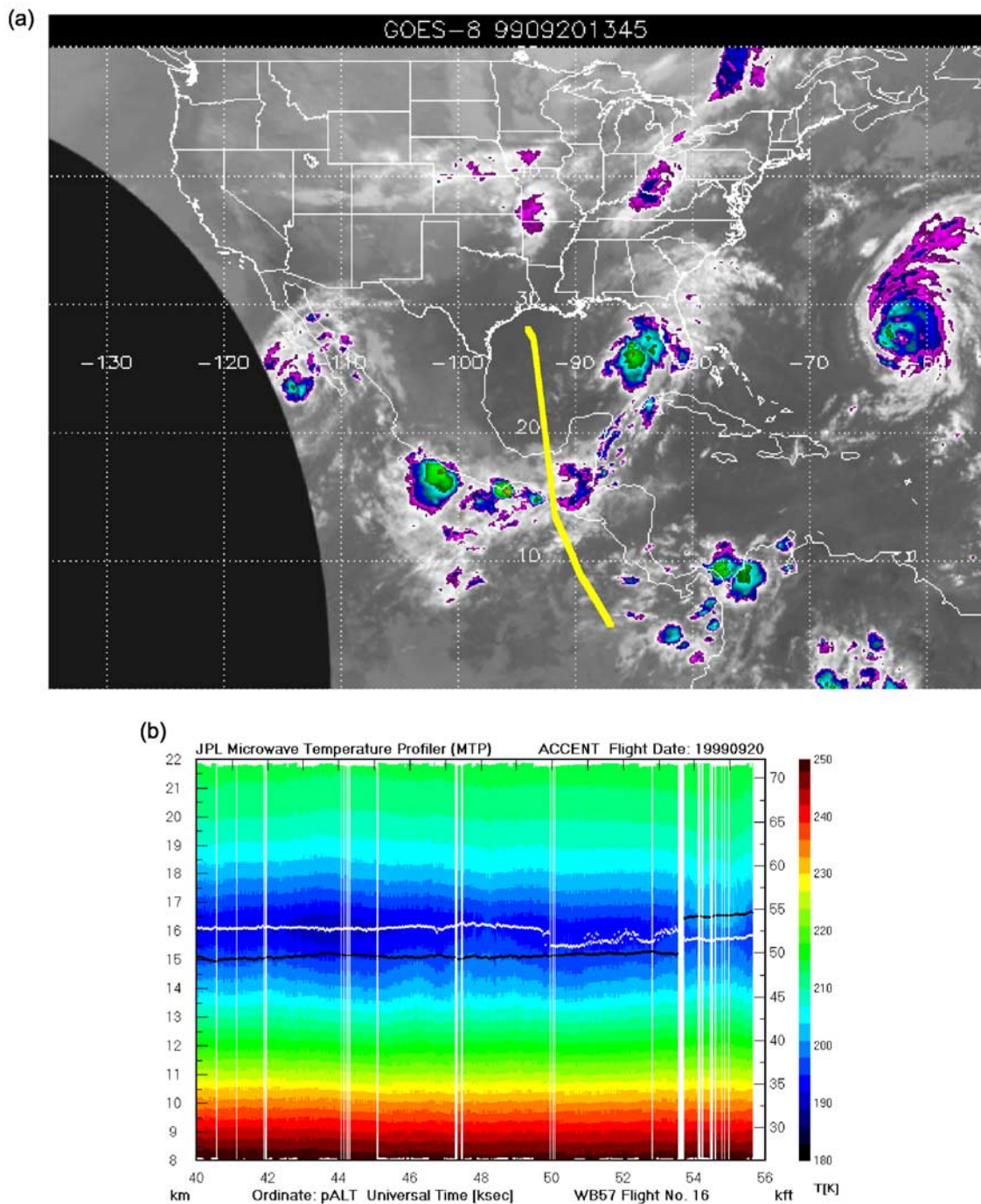


**Figure 2.** (a) GOES-8 IR image with WB57F flight track (yellow), 199909201345 UTC. Cloud top temperatures are color coded every 10 K down from 238 K. (b) Corresponding WB57F flight track (black trace) and tropopause (white trace) shown on the Microwave Temperature Profiler (MTP) temperature field.

There is a quite compact scatterplot with methyl iodide, the carbon monoxide shows a negatively correlated population accompanied by a positive one, methane shows a broad positive correlation which contains different sub-populations, while nitrous oxide and sulfur hexafluoride are very similar, showing a broad negative population accompanied by another in which approximately constant 30 ppbv of ozone spans the whole dynamic range of both  $\text{N}_2\text{O}$  and  $\text{SF}_6$ . The methyl iodide and carbon monoxide scatterplots estab-

lish short timescales for ozone. The broad positive correlation with methane is perhaps surprising, and the negative correlation with nitrous oxide and sulfur hexafluoride does argue for a long term stratospheric effect, with however no discrimination between tracers with lifetimes of  $10^2$  and  $10^3$  years. The positive  $\text{O}_3$ – $\text{CH}_4$  correlation would seem to preclude simple interpretations in terms of large-scale uplift from the planetary boundary layer with descent in the subtropical anticyclones yielding a negative correlation

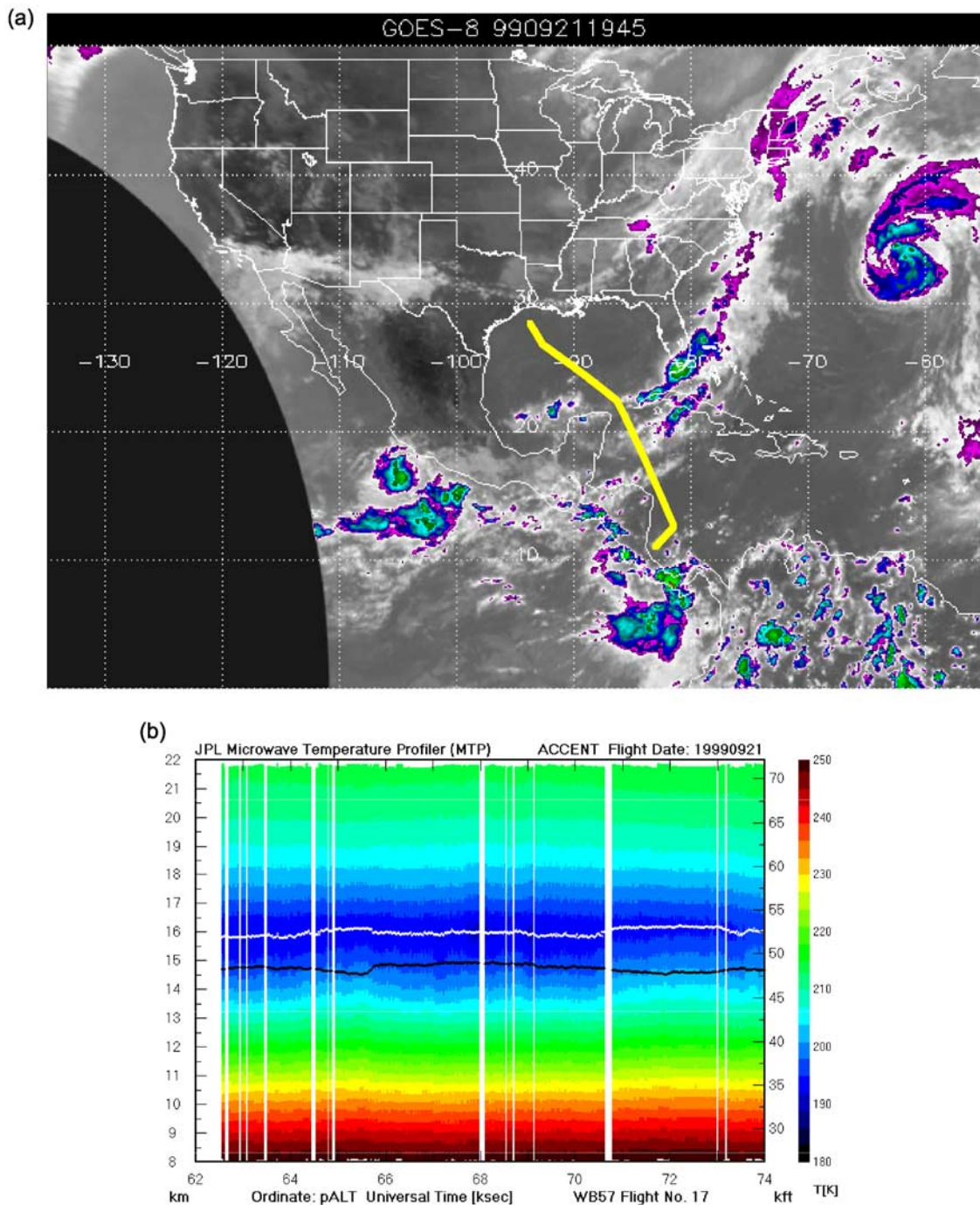


**Figure 3.** (a) GOES-8 IR image with WB57F flight track (yellow), 199909211945 UTC. Cloud top temperature is color coded every 10 K down from 238 K. (b) Corresponding WB57F flight track (black trace) and tropopause (white trace) shown on the MTP temperature field.

between methane with its surface source and ozone with its stratospheric source.

[12] We note that the large positive spike of the short-lived tracer of continental surface air, n-pentane (section 3.4), was accompanied by  $\sim 60$  ppbv of ozone and  $\sim 6$  ppmv of total water. While this is a reasonable value for ozone in a continental boundary layer, the water mixing ratio is indicative of rapid local dehydration in the upper tropical troposphere, since the lifetime of n-pentane is 2 days or less. Note that while supersaturation is present along parts of both

flights, we can say nothing about whether or not cirrus crystals were contributing to the total water mixing ratio.

[13] The minimum value of 3.8 ppbv of ozone occurred during a 1900s interval early in the flight of 19990921, between 61300 and 63200 s UTC (Coordinated Universal Time), when the ozone fluctuated between 4 and 40 ppbv, and was less than 20 ppbv much of the time (Figure 7). The lowest ozone mixing ratios were correlated with a period of elevated  $\text{CH}_4$  ( $>1750$  ppbv) and low  $\text{SF}_6$  ( $<4.2$  pptv), which included the final 1.5 km of the ascent from San Jose ( $10^\circ\text{N}$ ,



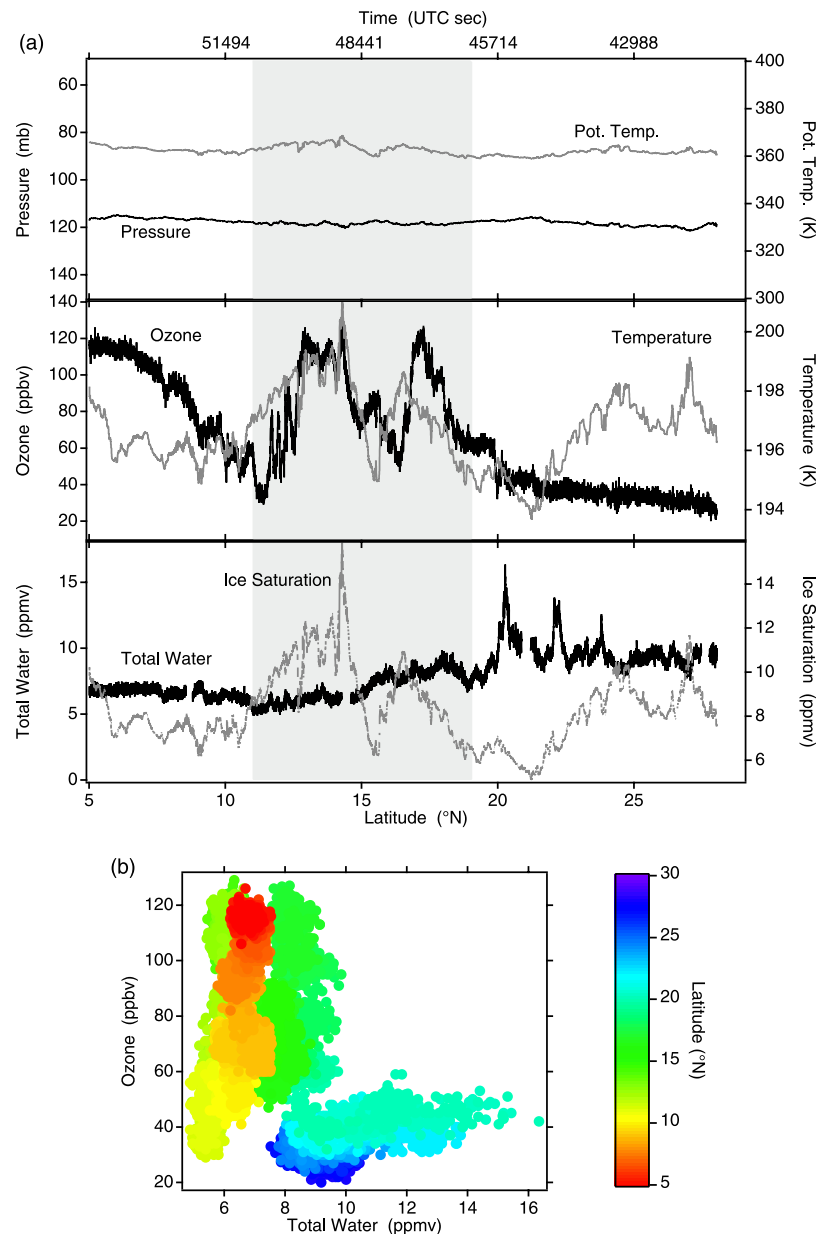


**Figure 4.** (a) Temperature, total water, and  $O_3$  along the flight track, end ascent: minimum latitude, 19990920. Gray shading shows approximate location of ITCZ. (b) Corresponding scatterplot.

86°W) and continued to (12.5°N, 82°W), or 63200 s UTC, at the 15 km cruise altitude.

### 3.2. Long-Lived Tracers: Methane, Nitrous Oxide, Sulfur Hexafluoride and Dichlorodifluoromethane (CFC-12)

[14] Figure 8a shows the time traces for methane, nitrous oxide and sulfur hexafluoride on 19990920, and Figure 8b shows the same data for 19990921. For 19990920 the LACE nitrous oxide varies between 313 and 316 ppbv; this variability is within the instrument noise level, and may be compared with a global mean surface mixing ratio of 314.8 ppbv for during September 1999. Ascent from 50,000 ft to 61,000 ft at 5°N northbound on 19990920 led to a stratospheric segment to 10°N. The nitrous oxide dropped to 309 ppbv in the stratosphere. Thus from the point of view

of a tracer with a surface source, a stratospheric sink and a 120-year atmospheric lifetime, the air encountered during the two flight legs 1–2 km below the tropical tropopause was tropospheric. There may however be a problem with the LACE nitrous oxide observations during aircraft climbout after takeoff, in that during ascent from Houston on 19990920 its mixing ratio went from 298 to 315 ppbv; the values <305 ppbv in the free troposphere are not consistent with any other species observed from the aircraft. There is some evidence that there is a problem with LACE measurements early in WB57F flights, arising from instrument environment temperature. Methane, however, with a 9-year lifetime shows a small but distinct latitudinal gradient, from a minimum ~1720 ppbv at 25°N to a maximum ~1780 ppbv at 5°N. The LACE data were in excellent agreement, rising from ~1720 to ~1780 ppbv. Sulfur hexafluoride, with a

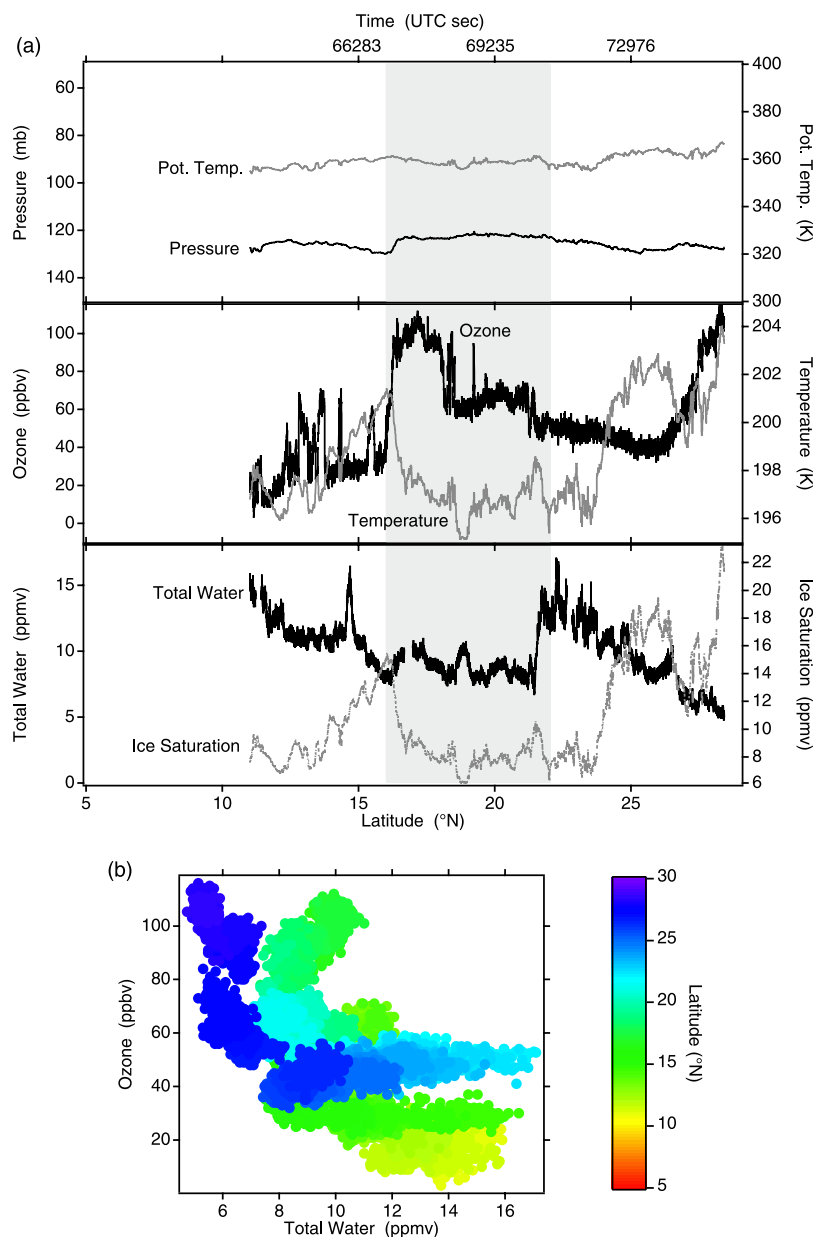


**Figure 5.** (a) Temperature, total water, and  $O_3$  along the flight track, end ascent: begin descent, 19990921. Gray shading shows approximate location of ITCZ. (b) Corresponding scatterplot.

positively increasing time trend, a primarily northern hemispheric surface source and a sink estimated to give a lifetime of thousands of years, shows a decrease south of  $\sim 13^\circ\text{N}$ . On the basis of these long-lived tracers, we might identify the air on 19990920 as tropospheric, with NH air from  $29^\circ\text{N}$  to  $19^\circ\text{N}$ , SH influenced air from  $9^\circ\text{N}$  to  $5^\circ\text{N}$ , with the ITCZ between. This latter assignment is consistent with the position of the high cloud on the satellite image in Figure 3. The CFC-12 from the WAS shows a general level of  $\sim 540$  pptv, with a fall to 528 pptv in the stratosphere. There are two minima, at either edge of the ITCZ, of 524 and 527 pptv, separated by a region of  $\sim 545$ – $552$  pptv in the ITCZ. The two lows coincide with minima in LACE CO (30–35 ppbv) and high ozone of 100–110 ppbv, and are present in two or more consecutive cans (Figure 8c). These observations suggest some fractional admixture of stratospheric air at these locations.

[15] The absolute values of the long-lived tracers at the surface for September 1999 which are archived at NOAA/CMDL are 535.1 and 530.0 ppbv ( $\text{CCl}_2\text{F}_2$ ), 4.51 and 4.21 pptv ( $\text{SF}_6$ ), 314.7 and 314.8 ppbv ( $\text{N}_2\text{O}$ ) and 1767 and 1717 ppbv ( $\text{CH}_4$ ) respectively at Mauna Loa ( $20^\circ\text{N}$ ,  $158^\circ\text{W}$ ) and American Samoa ( $14^\circ\text{S}$ ,  $171^\circ\text{E}$ ). We cannot invoke solely the admixture of some tropospheric SH air into the air sampled along the UTT flight tracks from  $29^\circ\text{N}$  to  $5^\circ\text{N}$  on 19990920 and 19990921 in order to explain the observed mixing ratios. The  $\text{SF}_6$  in particular suggests that there is probably some fraction, perhaps  $\sim 10\%$ , of formerly stratospheric air 1–2 km below the tropical tropopause.

### 3.3. Intermediate Lifetime Tracers: Methyl Chloride, Methyl Bromide, Carbon Monoxide, and Ethane

[16] Methyl chloride shows small variation along the 19990920 flight track in the upper tropical troposphere



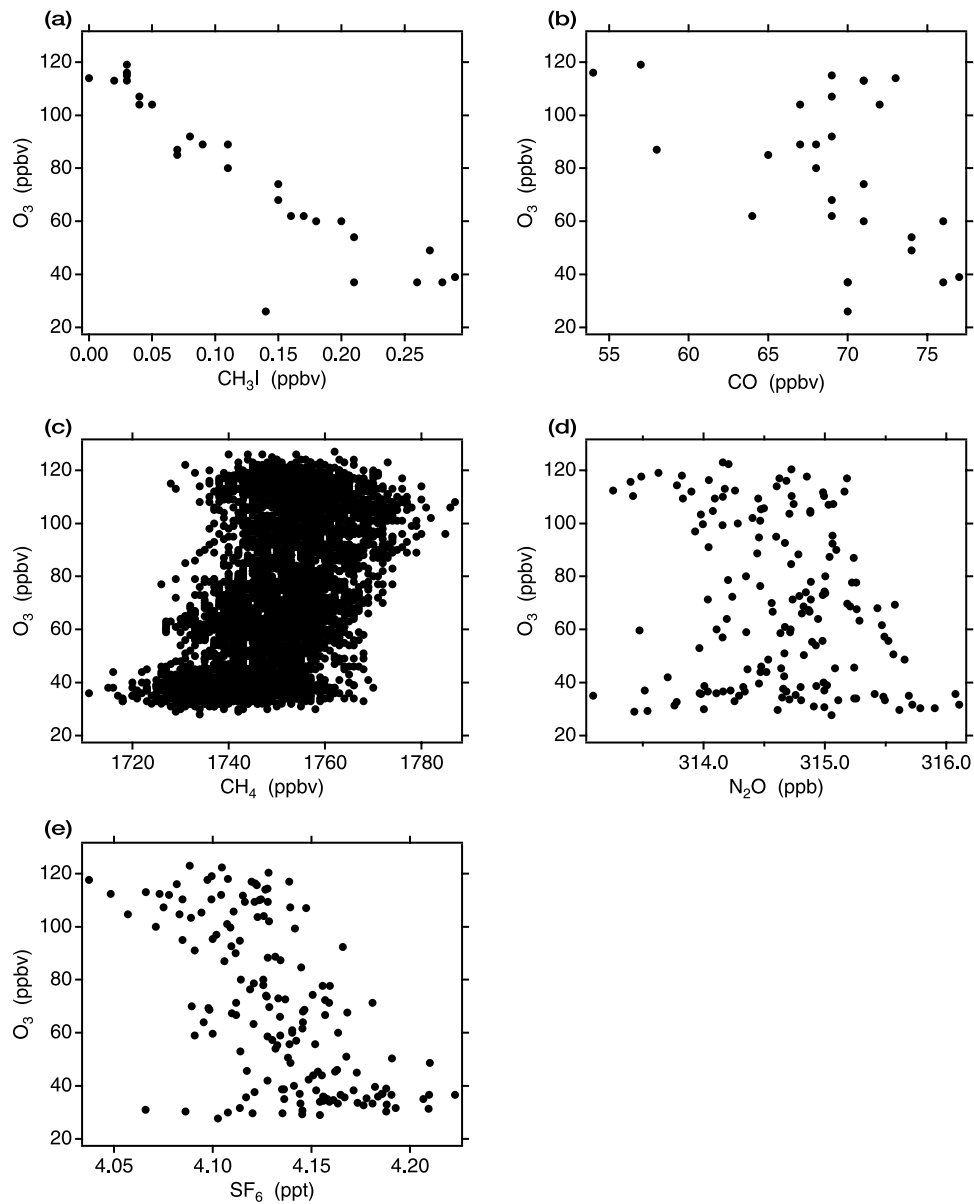


**Figure 6.** Some scatterplots for 19990920: (a)  $\text{O}_3$ ,  $\text{CH}_3\text{I}$  (WAS). (b)  $\text{O}_3$ ,  $\text{CO}$  (WAS). (c)  $\text{O}_3$ ,  $\text{CH}_4$  (NOAA/AL). (d)  $\text{O}_3$ ,  $\text{N}_2\text{O}$  (LACE). (e)  $\text{O}_3$ ,  $\text{SF}_6$  (LACE). The lifetimes of the molecules plotted versus  $\text{O}_3$  increase from  $10^{-2}$  to  $10^3$  years (Figure 6a–Figure 6e).

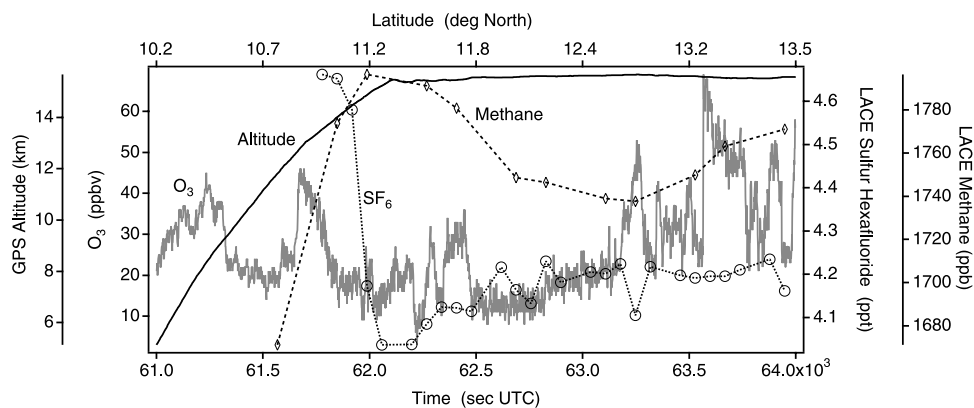


**Figure 7.** Ozone,  $\text{CH}_4$ ,  $\text{SF}_6$ , and altitude, 19990921, showing the ascent from San Jose ( $10^\circ\text{N}$ ,  $86^\circ\text{W}$ ) and the first 2000 s of horizontal cruise toward Ellington Field ( $30^\circ\text{N}$ ,  $95^\circ\text{W}$ ).

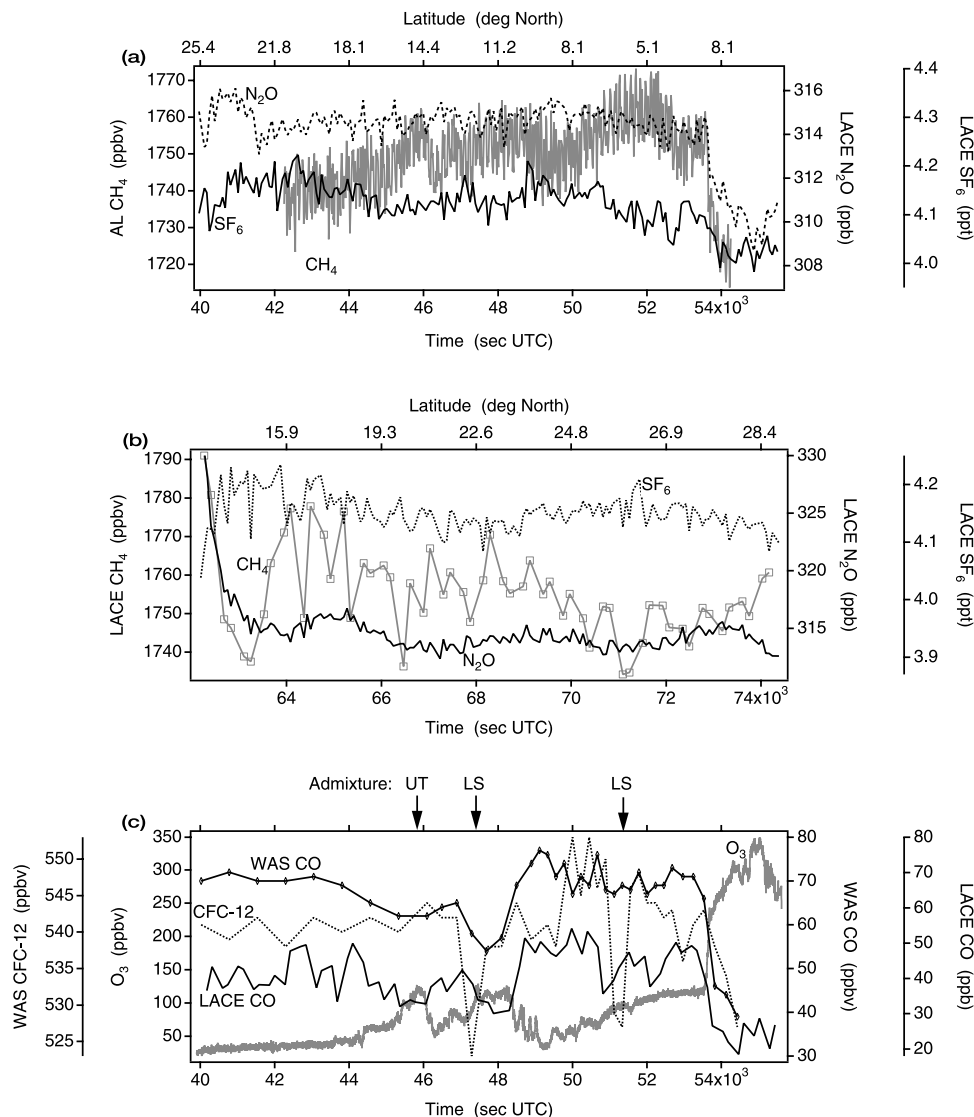


**Figure 8.** CH<sub>4</sub>, NOAA-CMDL N<sub>2</sub>O, and SF<sub>6</sub>, end ascent to begin descent. (a) 19990920 with NOAA-AL CH<sub>4</sub>, averaged from 0.5 Hz to 0.0625 Hz. (b) 19990921, with NOAA-CMDL CH<sub>4</sub>. (c) 19990920, whole air sampling (WAS) CCl<sub>2</sub>F<sub>2</sub>, and CO, with LACE CO and NOAA-AL O<sub>3</sub>.

(Figure 9a), with values of  $\sim 550$  pptv north ( $19^{\circ}$ – $25^{\circ}$ N) of the ITCZ region, and  $\sim 570$  pptv south ( $5^{\circ}$ – $9^{\circ}$ N). These are close to the mean tropospheric surface air values for this gas reported for the month, which has a  $\sim 1.5$  year lifetime. Methyl bromide, with a 0.8 year lifetime, shows markedly different behavior. It decreases from  $\sim 10.5$  pptv at  $25^{\circ}$ N to  $9.9$  pptv at the northern edge of the ITCZ ( $19^{\circ}$ N) shows a sharp increase in the ITCZ with a peak of  $10.6$  pptv and a decline south of the ITCZ ( $5^{\circ}$ – $9^{\circ}$ N) to variable values with a low of  $9.7$  pptv. Of the tracers considered so far, it is the first to show structure clearly related to that of ozone, mostly an anticorrelation. Carbon monoxide, with a lifetime of 0.4 years also shows a clear negative correlation with ozone over substantial segments of flight track, showing values below  $40$  ppbv in the locations of the ozone peaks reaching  $120$  ppbv at  $13^{\circ}$ N and  $17^{\circ}$ N, in the ITCZ (Figure 9b). Absolute values of CO of  $30$ – $40$  ppbv are well below values seen in the lower troposphere, and indicate both the local operation of a chemical sink and

some fractional presence of formerly stratospheric air; large amounts of stratospheric air, which has low CO content, are ruled out by the long-lived tracers but are consistent with about a 10% admixture. Ethane, with a lifetime of 0.2 years, shows a positive correlation with ozone north of and inside the ITCZ but south of it has a very large spike in excess of  $650$  pptv at  $\sim 9^{\circ}$ N which has little or no correlation with ozone. It is where the decrease in SF<sub>6</sub> begins (Figure 8a) and corresponds with spikes in *i*-butane and *n*-pentane, see next section.

### 3.4. Short Lifetimes: Methyl Iodide, *n*-Pentane and *i*-Butane

[17] The first two of these gases have lifetimes of order 0.01 years, and show similar but not identical correlations with ozone (Figure 10). Methyl iodide, with a natural marine source, is negatively correlated with ozone on the 19990920 flight segment while *n*-pentane, with an anthropogenic source, is negatively correlated with ozone north of



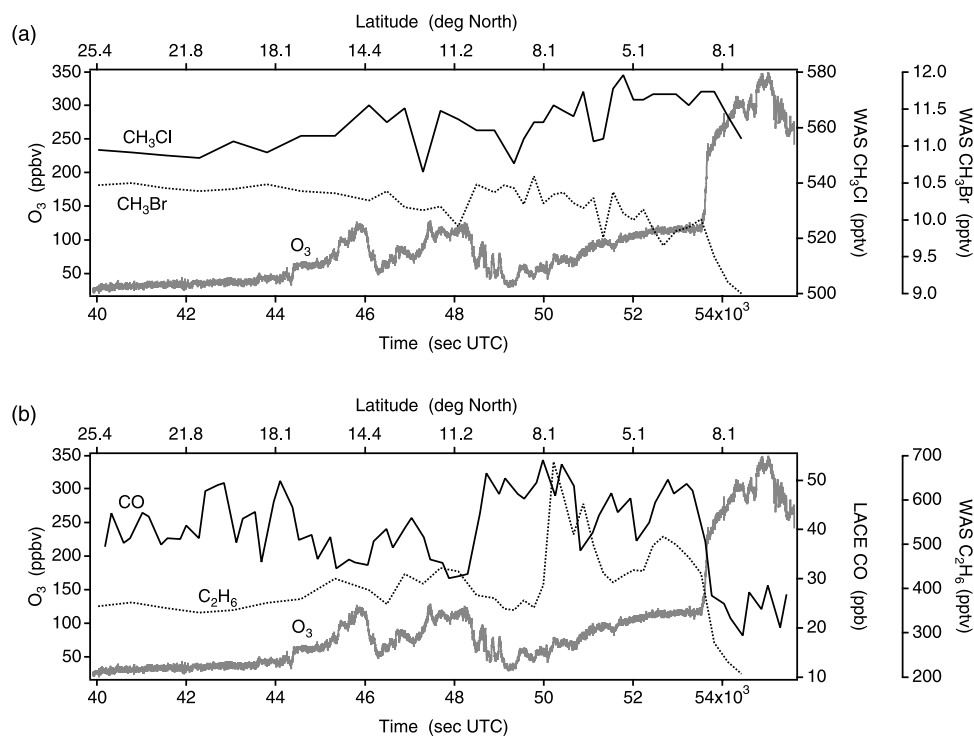


**Figure 9.** (a)  $O_3$  with WAS  $CH_3Cl$  and  $CH_3Br$ , end ascent to begin descent, 19990920. (b)  $O_3$  with LACE CO and WAS  $C_2H_6$ , end ascent to begin descent, 19990920.

and in the ITCZ, and has a large spike south of it co-located with the positive spike in ethane which shows no correlation with ozone. The third gas, i-butane, has a lifetime of  $\sim 0.02$  years, and correlates well with both ethane and n-pentane, as it should with an anthropogenic source.

### 3.5. Vertical Profiles Near Houston ( $30^\circ N$ , $95^\circ W$ ) and San Jose ( $10^\circ N$ , $86^\circ W$ )

[18] The vertical profiles from LACE on 19990921 (Figure 11) show at both ends of the flight that both  $SF_6$  and CO were considerably more abundant in the lower troposphere ( $\sim 4.6$  pptv and  $>100$  ppbv) than they were at flight level in the upper troposphere, ( $\sim 4.1$  pptv and  $<55$  ppbv) respectively. This observation is consistent with

the values measured at the surface at Mauna Loa and American Samoa by the NOAA/CMDL network, and with airborne results in *Flocke et al.*, [1999] and *Schaffler et al.*, [1999]. The WAS observations of CO have been validated against independent infrared tunable diode laser measurements on the ER-2 [*Flocke et al.*, 1999].

### 3.6. Correlations With Particle Analysis by Laser Mass Spectrometry Observations of Particle Composition

[19] The particle analysis by laser mass spectrometry (PALMS) instrument can obtain mass spectra of individual aerosol particles in near real time on the WB57F aircraft [*Murphy et al.*, 1998]. No PALMS analyses were considered when the WB57F was in cirrus cloud, because of the

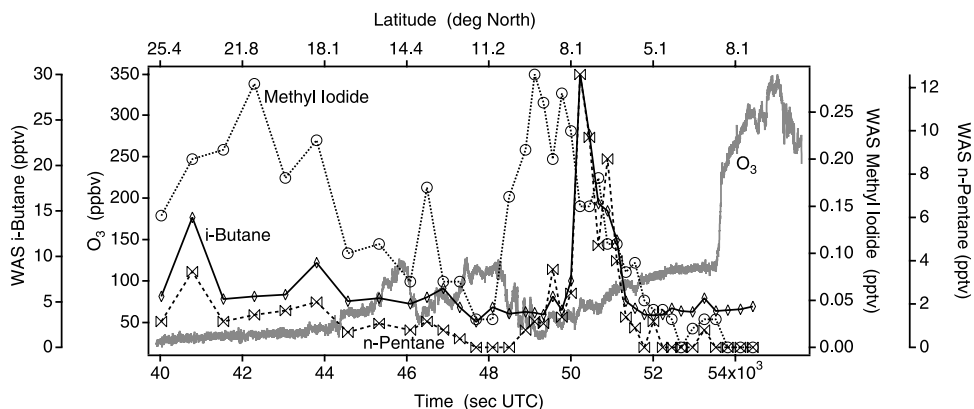


**Figure 10.**  $O_3$  with WAS methyl iodide, i-butane, and n-pentane, end ascent to begin descent, 19990920.

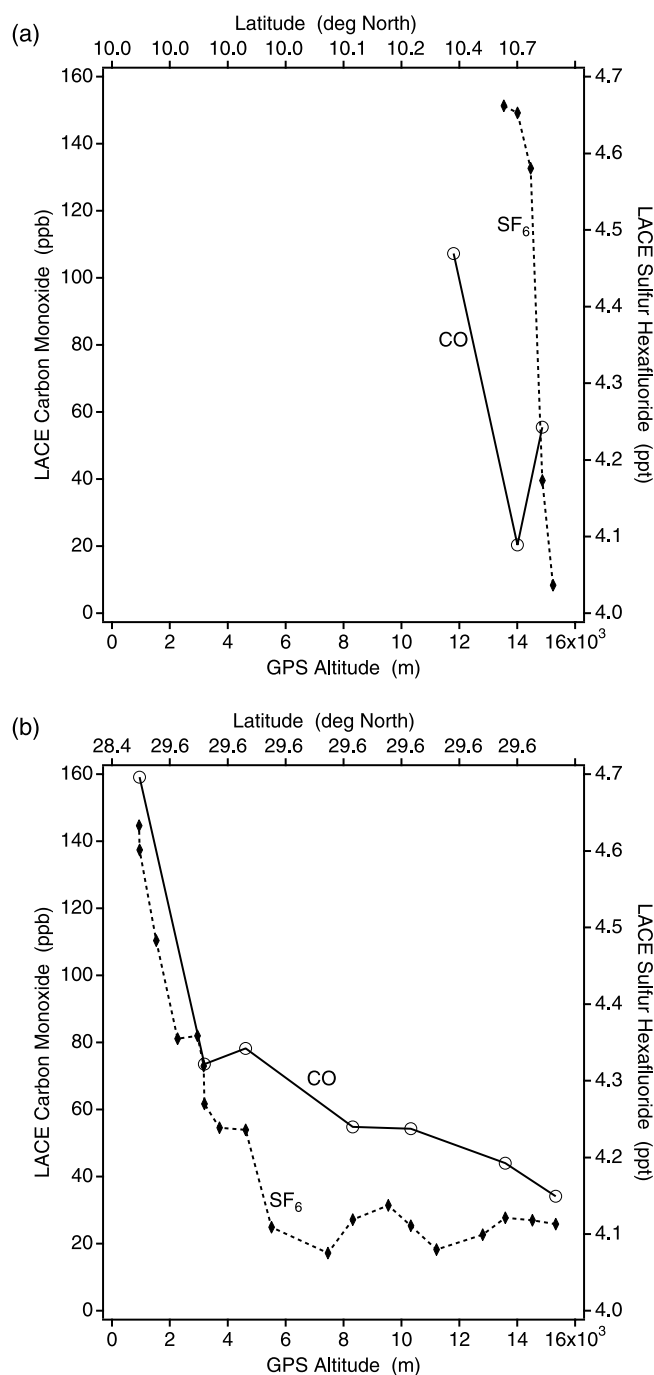


**Figure 11.** Vertical profiles of LACE CO and SF<sub>6</sub>, 19990921. (a) Take off to end ascent. (b) Begin descent to land. A single observation of zero or negative CO has been removed from this figure.

possibility that ice crystal impacts on the inlet walls could yield mass spectra characteristic of the inlet surfaces rather than the atmosphere. For this reason, based on the appearance of artifacts in the PALMS data in regions saturated with respect to ice, spectra were eliminated from 44,000 to 46,000 UTC s on 19990920 and over substantial sections of the flight track on 19990921. Figure 12 shows the types of particles encountered during various portions of the flights. Here the data have been simplified by using a hierarchical

cluster analysis to group similar particles [Murphy *et al.*, 2003]. Some of the categories, such as meteoric, are quite distinct whereas some of the others, such as the organic sulfate mixtures, represent divisions among a continuum of composition. Short gaps in the PALMS data are due to negative ion mode and the longer gaps are due either to laser realignment or to removing data that could possibly be in clouds.

[20] We will consider the correlation of the PALMS data on these flights with the gaseous species discussed in sections 3.1–3.4. The PALMS spectra provide additional evidence of the complex mixing processes suggested by the gas phase species and discussed throughout this paper. For example, on 19990921 there are two regions of frequent particles containing MSA: between 24°N and 27°N and near 16°N. Yet the pattern of the organic/sulfate particles in the two regions is very different: near 16°N many of the sulfate and organic particles fit the category third from the bottom on the graph whereas this category is almost entirely absent near 26°N. The relative contributions of the bottom three categories are also very different on 19990920 near 5.5°N and 14°N, even though both regions have ~110 ppbv of O<sub>3</sub>.

[21] Figure 13a shows the relative amounts of organic and sulfate ions in the negative ion spectra for the horizontal transects on these two flights. Sulfuric acid and ammonium sulfate are both efficient at producing negative ions (mostly HSO<sub>4</sub><sup>-</sup>), so the ion fractions should be viewed as an upper limit on the aerosol sulfate concentration and a lower limit on the aerosol organic concentration.

[22] Consistent with earlier flights [Murphy *et al.*, 1998], the stratospheric aerosol is mostly sulfate. Sulfate and organic ion fractions can be comparable in some of the upper troposphere. What is unusual here is that the particles in air with less than ~60 ppbv of O<sub>3</sub> have a low organic content. The ~0.1 fraction of organic ions is much lower than most tropospheric air sampled in the midlatitude free troposphere, including some data at low altitude over the Pacific Ocean west of California. Not only that, the organics present in low-ozone air have a distinct composition, as indicated by the negative correlation between O<sub>3</sub> and positive ion 45, most probably HCO<sub>2</sub><sup>+</sup> (Figure 13b). One explanation for the low organic content is that the low O<sub>3</sub> air on these flight segments originated in part from an unpolluted marine boundary layer. Mercury was almost entirely absent when O<sub>3</sub> was >50 ppbv, indicating little contact of such air with the tropopause region [Murphy *et al.*, 1998].

[23] The high concentration of spectra between 24°N and 27°N indicative of MSA on 19990921 is very unusual compared to other flights of the PALMS instrument. Figure 13b shows the relationship between O<sub>3</sub> and the positive 97 peak indicative of MSA. The strong anti-correlation indicates that some of the low-O<sub>3</sub> air originated from the marine boundary layer. This explanation is consistent with the strong anti-correlation between O<sub>3</sub> and CH<sub>3</sub>I (section 3.4). The high sulfate in the low-ozone air could then come from oxidation of dimethyl sulfide (DMS).

[24] A number of other features are evident in the categorization. Spectra rich in potassium are more common equatorward of 9°N, indicating a probable larger contribution of biomass burning to the particles there. There is a small but persistent fraction of particles with a meteoric



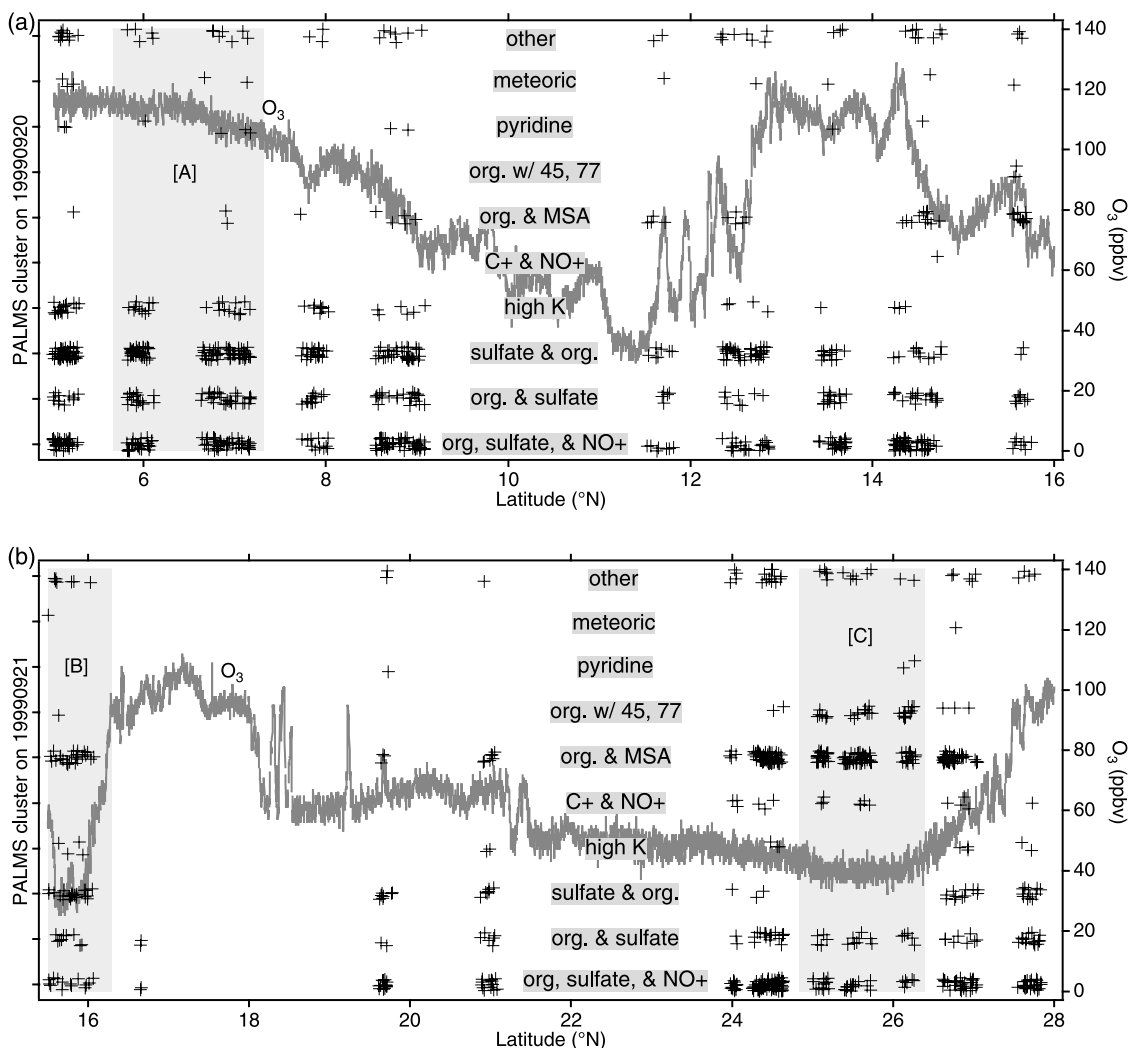


**Figure 12.** Particle analysis by laser mass spectrometry positive ion spectra on (a) 19990920 and (b) 19990921. Each point represents a single mass spectrum assigned to a category. The small vertical spread within each category is just random noise added in order to reduce the number of overlapping symbols on the graph. The order of the categories is arbitrary although some effort has been made to put similar categories next to each other on the graph.

signature indicative of gravitational settling and exchange of particles from the stratosphere. Some sections of flight include both biomass burning and stratospheric particles, indicating mixing of surface and stratospheric air. There is also a low background of spectra with a large, isolated peak at 80 which we tentatively identify as protonated pyridine [Schulte and Arnold, 1990].

### 3.7. Three-Dimensional Back Trajectories

[25] Although air parcel back trajectories originating in the upper tropical troposphere, calculated from numerical weather prediction suites, cannot be expected to convey the effects of deep convection accurately on the scale of cumulonimbus towers, they can provide useful qualitative information about air mass origins on horizontal scales larger than the grid resolution ( $1^\circ \times 1^\circ$  in this case). They can, of course, say nothing about smaller-scale mixing. Five-day back trajectories from along the flight track on 19990920 in Figure 14a generally showed that north of

$10^\circ\text{N}$  the sampled air parcels were in a large anticyclonic circulation centered over the Gulf of Mexico at about ( $25^\circ\text{N}$ ,  $90^\circ\text{W}$ ). This was also true for the sampled air on the following day from  $\sim 13^\circ\text{N}$  (Figure 14b). The trajectories south of these latitudes had been in generally easterly flow during the 5 days prior to being sampled. On 19990920 virtually all the back trajectories showed descent during the previous 1–2 days, but several trajectories ending near the ITCZ did show ascent from altitudes up to 3 km lower than the flight track on timescales in the 2–5 day range. One ascended from a midlatitude stratospheric location at about ( $43^\circ\text{N}$ ,  $65^\circ\text{W}$ ). This behavior is compatible with the low  $\text{CCl}_2\text{F}_2$  spikes recorded by WAS, along with the low CO and relatively high  $\text{O}_3$  in Figure 8c. The early part of the flight of 19990921 was marked by low-ozone mixing ratios, often  $<20$  ppbv and reaching a minimum of 3.8 ppbv, accompanied by elevated methane and low  $\text{SF}_6$ . The 5-day back trajectories originate from an area located at ( $15\text{--}22^\circ\text{N}$ ,  $55\text{--}60^\circ\text{W}$ ), and show marked

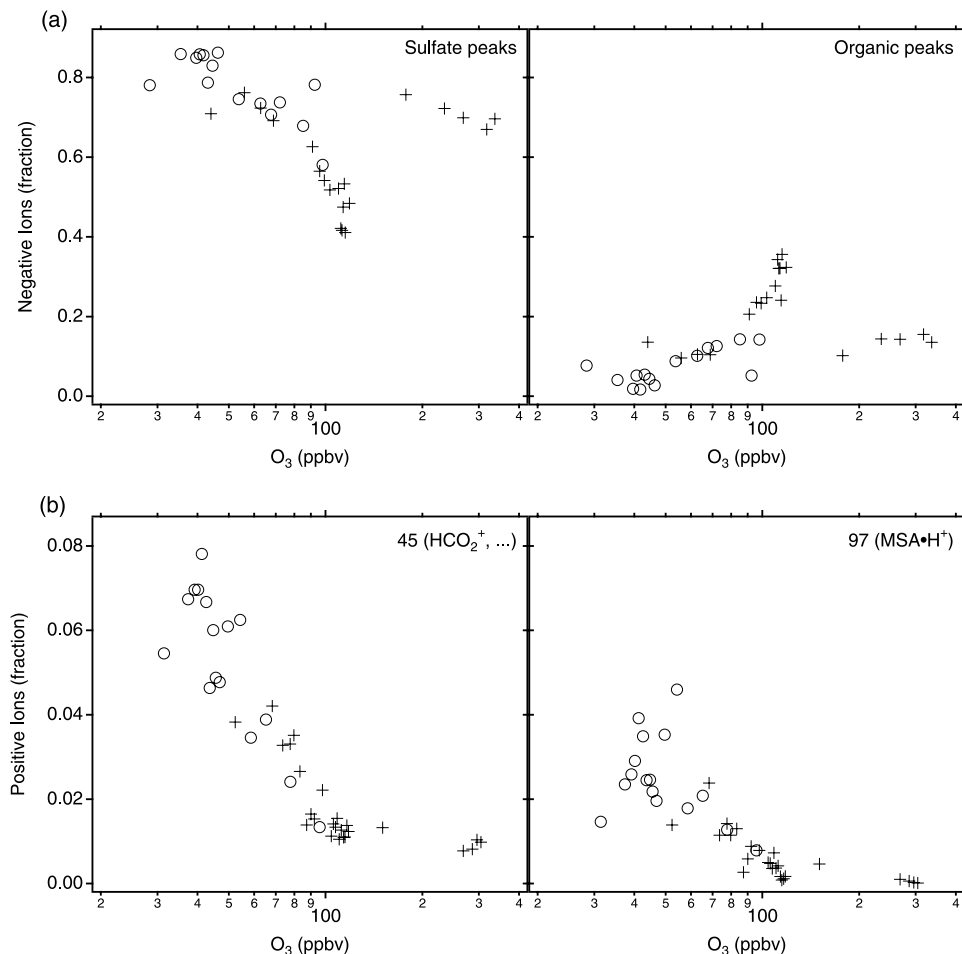


**Figure 13.** (a) Average intensity of the sum of several negative ion organic and sulfate peaks as a function of  $O_3$ . Each point represents an average of  $\sim 40$  particles with plus signs representing data on 20 September and circles data on 21 September. The  $O_3$  scale has been made logarithmic to compress the stratospheric data. (b) Average intensity of mass 45 and 97 positive ions. Mass 45 is probably mostly  $HCO_2^+$  and 97 mostly protonated MSA.

ascent 4–5 days previously (Figure 14). The area is not marked by evidence of deep convection on satellite images during the 19990915–19990921 period. An ozone sonde ascent [Thompson *et al.*, 2003] from Paramaribo (6°N, 55°W) on 19990915 does show low ozone (15 ppbv) at the surface, but has 50–70 ppbv throughout the free troposphere. Recent descent was not as marked on 19990921, but trajectories from both north and south of the ITCZ showed descent from above 14.5 km, in particular the final segments of the flight track near Ellington Field (30°N, 95°W), which are consistent with the low water, high ozone, that is to say stratospheric, population in Figure 5b.

[26] The values of  $\dot{\theta}$  implied by the 5-day, 3-dimensional trajectories were significant, particularly when translated into altitude changes in the troposphere, and preclude extension back to 10 days. It should be noted that some longer isentropic back trajectories do lead back to the general vicinities of Hurricanes Floyd and Gert, particularly for 19990920, but that with our present analysis this cannot be regarded as an established result. In particular, we do not regard quantitative assessment of fluxes of mass or tracers as feasible via Lagrangian transport.

[27] The ranges, averages and standard deviations of meteorological and chemical variables over the horizontal flight tracks in the upper troposphere for the two flights are shown in Table 1. The ranges and standard deviations carry more information than the means, although the latter are probably what would be comparable with large-scale model results. The wind speed, temperature, total water and ozone have been shown elsewhere to be statistical multifractals with the characteristics of generalized-scale invariance [Tuck *et al.*, 2003].

#### 4. Discussion

[28] These new flights 1–2 km below the tropical tropopause offer a complicated picture there of ozone and of its correlation with other species possessing a range of lifetimes from  $10^{-2}$  to  $10^3$  years. The only species showing a (negative) correlation with ozone sustained over the entire flight segment from 29°N to 5°N was methyl iodide, which has a marine source and a lifetime of  $\sim 3$  days. This suggests that the ozone in the upper tropical troposphere was significantly affected by marine convection on this timescale over the entire flight

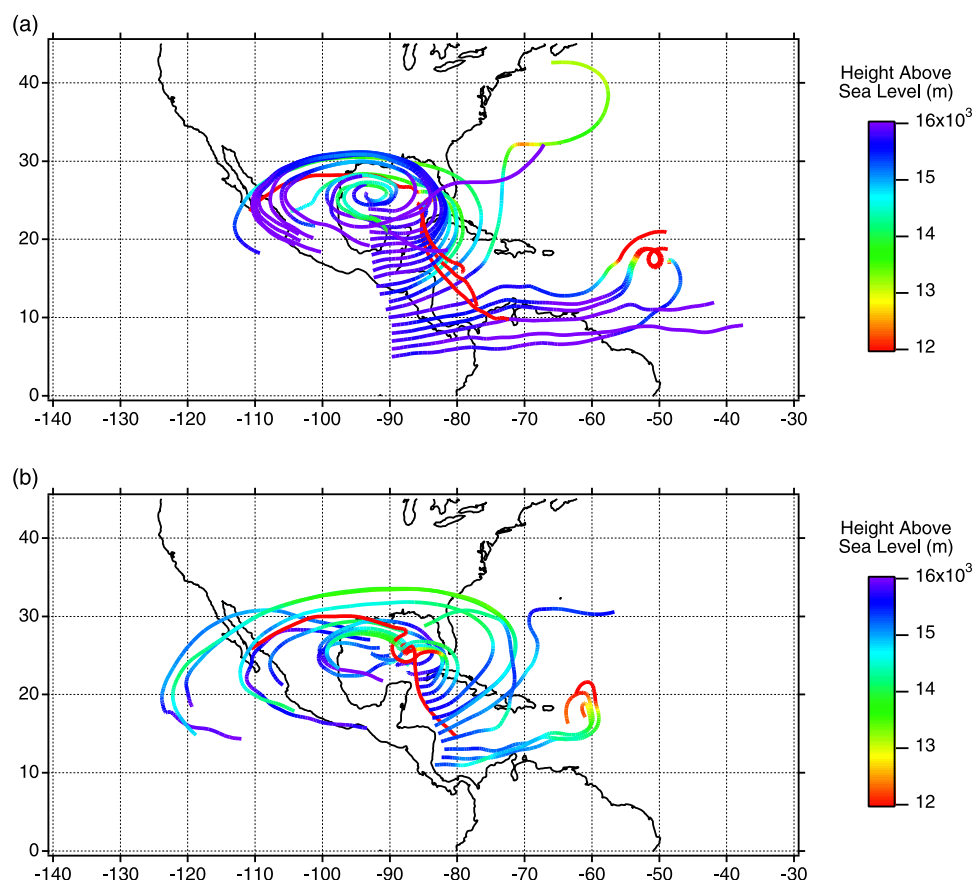


**Figure 14.** Five-day back trajectories from along the WB57F flight tracks of (a) 19990920 and (b) 19990921, calculated in three dimensions from 6-hourly European Centre for Medium-Range Weather Forecasts analyses. The color coding shows the pressure altitude history of the air parcels; each trajectory is representative of a larger population whose paths are not shown in the interests of clarity.

segment; *Cohan et al.* [1999] have demonstrated that methyl iodide is a tracer of marine convection in middle levels (8–12 km) of the tropical troposphere. The short-lived hydrocarbons n-pentane (0.01 years) and i-butane (0.02 years) were negatively correlated with ozone north of and in the ITCZ, but uncorrelated with it south of there, particularly at the location of a large spike in all hydrocarbons there, including ethane with an order of magnitude longer lifetime (0.2 years). The values of carbon monoxide were well below general tropospheric levels, averaging  $\sim 40$  ppbv. Low CO excursions to  $\sim 30$  ppbv were anticorrelated with ozone, suggesting either ozone production via OH initiated oxidation of CO, or alternatively some mixed-in stratospheric air component or both. Although not evident in  $\sim 120$ -year lifetime  $N_2O$  from LACE, there are two negative spikes of  $CCl_2F_2$  (CFC-12) from WAS with lower stratospheric values at which ozone has mixing ratios (100–110 ppbv) which are greater than normal tropospheric values in the tropics. Finally, the period of low ozone early on the flight of 19990921 was most probably air from the marine boundary layer over the tropical Atlantic.

[29] The best interpretation appears to be that the upper tropospheric ozone 1–2 km below the tropical tropopause had identifiable influences from (1) marine convection:

**Table 1.** Ranges and Means for all Measurements Except the WAS Measurements Calculated by Concatenating the 19990920 Flight and the 19990921 Flight

| Variable             | Units | Range           | Mean $\pm$ StDev    |
|----------------------|-------|-----------------|---------------------|
| $C_2H_6$ (WAS)       | pptv  | 207.00–686.00   | $416.54 \pm 92.68$  |
| CFC-12 (WAS)         | pptv  | 523.00–553.00   | $540.72 \pm 6.38$   |
| $CH_3Br$ (WAS)       | pptv  | 9.00–10.59      | $10.15 \pm 0.36$    |
| $CH_3Cl$ (WAS)       | pptv  | 544.00–579.00   | $561.92 \pm 8.82$   |
| $CH_3I$ (WAS)        | pptv  | 0.00–0.29       | $0.12 \pm 0.09$     |
| $CH_4$ (AL)          | ppbv  | 1711.00–1790.00 | $1751.80 \pm 9.62$  |
| $CH_4$ (LACE)        | ppb   | 1722.50–1791.00 | $1752.50 \pm 13.10$ |
| CO (LACE)            | ppb   | 28.80–58.45     | $42.84 \pm 6.46$    |
| CO (WAS)             | ppbv  | 39.00–77.00     | $66.46 \pm 8.49$    |
| $SF_6$ (LACE)        | ppt   | 4.04–4.23       | $4.14 \pm 0.03$     |
| i- $C_4H_{10}$ (WAS) | pptv  | 2.80–30.20      | $6.86 \pm 5.72$     |
| n- $C_5H_{12}$ (WAS) | pptv  | 0.00–12.60      | $1.82 \pm 2.79$     |
| $N_2O$ (LACE)        | ppb   | 312.38–331.15   | $314.75 \pm 1.91$   |
| $O_3$                | ppbv  | 3.00–129.00     | $61.22 \pm 28.49$   |
| $H_2O$               | ppmv  | 4.74–17.10      | $8.79 \pm 2.20$     |
| Ice saturation       | ppmv  | 5.10–164.10     | $10.71 \pm 10.49$   |
| Pressure             | mb    | 114.81–129.92   | $121.51 \pm 4.29$   |
| Temperature          | K     | 193.65–204.04   | $197.64 \pm 2.01$   |

WAS, whole air sample; 19990920 flight, endascent-beginchgal; 19990921 flight, endascent-beginchgal; StDev, standard deviation; pptv, parts per trillion by volume. The WAS ranges and means reflect the 19990920 flight only.



low values with high  $\text{CH}_3\text{I}$  [Cohan *et al.*, 1999], (2) terrestrial convection: positive correlation in places with ethane, (3) in situ chemistry: negative correlation with  $\text{CO}$ ,  $\text{n-C}_5\text{H}_{12}$  and  $\text{i-C}_4\text{H}_{10}$ , and (4) stratospheric descent: high values at low  $\text{CCl}_2\text{F}_2$  values. These conclusions are consistent with evidence from the PALMS mass spectra of individual aerosols, which additionally showed the presence of biomass burning aerosols in both the upper troposphere and lower stratosphere, and the presence of methane sulfonic acid on aerosols whose abundance was negatively correlated with ozone. The signature of mercury in PALMS mass spectra indicates time spent near the tropical tropopause, and thus constitutes independent evidence for recirculation of air [Tuck *et al.*, 1997] between the upper troposphere and lower stratosphere in the tropics. There is independent evidence that the scaling of ozone on these flights suggests sources and sinks operating faster than mixing [Tuck *et al.*, 2003]. Ozone varied between 3 and 130 ppbv, consistent with intermingled air masses having disparate origins and in situ chemistries of different rates. We note that the large positive spike of hydrocarbons south of the ITCZ was not only accompanied by ozone of  $\sim 60$  ppbv, the total water content was among the lowest on the flight, at  $\sim 6$  ppmv. Since  $\text{n-C}_5\text{H}_{12}$  and  $\text{i-C}_4\text{H}_{10}$  have lives of only 1–3 days it implies that what must have been relatively moist surface continental air had been quickly dried to tropical tropopause and lower stratospheric values for the location and time of year. The negative-going spikes of lower stratospheric  $\text{CCl}_2\text{F}_2$  and  $\text{CO}$  near the ITCZ suggests that perhaps downdrafts or descending anvils have brought some air down across the tropical tropopause. Finally, these local results are in accord with the satellite-based global arguments of both Sassi *et al.* [2001] about upper tropospheric humidity and convection, and Clark *et al.* [2001] about the lack of evidence for the production of dehydrated air for the stratosphere at one location with subsequent advection elsewhere; here, as in Tuck *et al.* [1997], there is in situ evidence that water at and just above the tropical tropopause is locally determined.

[30] The 3D back trajectories (Figure 14) are generally consistent with the foregoing picture derived from consideration of the chemical species and their correlations. However, it must be noted that the small-scale variability implies that the observed molecular distributions cannot be interpreted in terms of simple large-scale concepts such as “up in the ITCZ, down in the subtropical anticyclones”. Quantitative descriptions of the transport of trace molecules appear not to be possible using current operational forecast models, in either Eulerian or Lagrangian frameworks.

[31] The question of how to lend coherence to small-scale structure has been addressed by Tuck *et al.* [2003], who employed generalized-scale invariance in treating the airborne time series of wind, temperature, ozone and total water as statistical fractals. It is clear that simple dynamical constructs such as large-scale Eulerian advection, or Lagrangian trajectories of a conserved large-scale air mass, cannot explain the multiscale variability, and therefore cannot explain the transport. The fat-tailed probability distributions yielded by the airborne data say that the means are influenced by a small number of intense events,

but that all scales are involved in the transport. The multifractal scaling exponents describing the conservation, intermittency and Lévy flight fields provide a quantitative description.

## 5. Conclusions

[32] Two hitherto unique WB57F flights 1–2 km below the tropical tropopause at constant pressure (and potential temperature) have shown that ozone there has influences from several different processes, which collectively produced a range of mixing ratios from 3 to 130 ppbv. Total water varied from 4 to 17 ppmv. Identifiable processes were recirculation, marine convection, continental convection, in situ chemical production, biomass burning and some downward admixture of lower stratospheric air. There was no large-scale division of these signatures into separate air masses. The processes were identified by local regions of correlation (positive and negative) with a variety of gaseous and particulate tracers whose lifetimes ranged from  $10^{-2}$  to  $10^3$  years. Ozone is affected by these processes on time-scales of days; the mixing and correlation is local [O'Neill, 1992]. As far as transport is concerned, the small-scale variation is not noise, it is music.

[33] **Acknowledgments.** We thank B. A. Ridley for valuable comments regarding the lowest ozone values. Research performed by MJM and RRF at the Jet Propulsion Laboratory, California Institute of Technology, was carried out under contract with the National Aeronautics and Space Administration. A unique review improved the paper.

## References

- Bethan, S., G. Vaughan, and S. J. Reid (1996), A comparison of ozone and thermal tropopause heights and the impact of tropopause definition on quantifying the ozone content of the troposphere, *Q. J. R. Meteorol. Soc.*, **122**, 929–944.
- Clark, H. L., A. Billingham, R. S. Harwood, and H. C. Pumphrey (2001), Water vapor in the tropical lower stratosphere during the driest phase of the atmospheric “tape recorder,” *J. Geophys. Res.*, **106**, 22,695–22,706.
- Cohan, D. S., M. G. Schultz, D. J. Jacob, B. G. Heikes, and D. R. Blake (1999), Convective injection and photochemical decay of peroxides in the tropical upper troposphere: Methyl iodide as a tracer of marine convection, *J. Geophys. Res.*, **104**, 5717–5724.
- Denning, R. F., S. L. Guidero, G. S. Parks, and B. L. Gary (1989), Instrument description of the airborne Microwave Temperature Profiler, *J. Geophys. Res.*, **94**, 16,757–16,766.
- Dessler, A. E., and S. C. Sherwood (2000), Simulations of tropical upper tropospheric humidity, *J. Geophys. Res.*, **105**, 20,155–20,163.
- Flocke, F., et al. (1999), An examination of the chemistry and transport processes in the tropical lower stratosphere using observations of long-lived and short-lived compounds obtained during STRAT and POLARIS, *J. Geophys. Res.*, **104**, 26,625–26,642.
- Folkens, I. R., M. Loewenstein, J. R. Podolske, S. J. Oltmans, and M. H. Proffitt (1999), A barrier to vertical mixing at 14 km in the tropics: Evidence from ozonesondes and aircraft measurements, *J. Geophys. Res.*, **104**, 22,095–22,102.
- Gettelman, A. J., J. R. Holton, and A. R. Douglass (2000), Simulations of water vapor in the lower stratosphere and upper troposphere, *J. Geophys. Res.*, **105**, 9003–9023.
- Herman, R. L., et al. (1998), Tropical entrainment timescales inferred from stratospheric  $\text{N}_2\text{O}$  and  $\text{CH}_4$  observations, *Geophys. Res. Lett.*, **25**, 2781–2784.
- Jensen, E. J., L. Pfister, A. S. Ackerman, A. Tabazadeh, and O. B. Toon (2001), A conceptual model of the dehydration of air due to freeze-drying by optically thin, laminar cirrus rising slowly across the tropical tropopause, *J. Geophys. Res.*, **106**, 17,073–17,496.
- Kelly, K. K., et al. (1989), Dehydration in the lower Antarctic stratosphere during late winter and early spring, 1987, *J. Geophys. Res.*, **94**, 11,317–11,357.
- Kelly, K. K., M. H. Proffitt, K. R. Chan, M. Loewenstein, J. R. Podolske, S. E. Strahan, J. C. Wilson, and D. Kley (1993), Water vapor and cloud

- measurements over Darwin during STEP 1987 tropical mission, *J. Geophys. Res.*, **98**, 8713–8724.
- Ludlam, F. H. (1980), *Clouds and Storms: The Behavior and Effect of Water in the Atmosphere*, ch. 8.6, pp. 228–231, Penn. State Univ. Press, University Park, Penn.
- Moore, F. L., et al. (2003), Balloonborne in situ gas chromatograph for measurements in the troposphere and stratosphere, *J. Geophys. Res.*, **108**(D5), 8330, doi:10.1029/2001JD000891.
- Murgatroyd, R. J. (1965), Ozone and water vapor in the upper troposphere and lower stratosphere, in *Meteorological Aspects of Atmospheric Radioactivity*, pp. 68–94, Rep. 169, World Meteorol. Organ., Geneva.
- Murphy, D. M., D. S. Thomson, and M. J. Mahoney (1998), In situ measurements of organics, meteoritic material, mercury, and other elements in aerosols at 5 to 19 km, *Science*, **282**, 1664–1669.
- Murphy, D. M., A. M. Middlebrook, and M. Warshawsky (2003), Cluster analysis of data from the Particle Analysis by Laser Mass Spectrometry (PALMS) instrument, *Aerosol Sci. Technol.*, **37**, 382–391.
- O'Neill, T. P., Jr. (1992), *All Politics is Local*, 208 pp., Adams Media, New York.
- Proffitt, M. H., M. J. Steinkamp, J. A. Powell, R. J. McLaughlin, O. A. Mills, A. L. Schemmtekopf, T. L. Thompson, A. F. Tuck, T. Tyler, and R. H. Winkler (1989), In situ ozone measurements within the 1987 Antarctic ozone hole from a high-altitude ER-2 aircraft, *J. Geophys. Res.*, **94**, 16,547–16,555.
- Richard, E. C., K. K. Kelly, R. H. Winkler, R. Wilson, T. L. Thompson, R. J. McLaughlin, A. L. Schemmtekopf, and A. F. Tuck (2002), A fast-response near-infrared tunable diode laser absorption spectrometer for in situ measurements of CH<sub>4</sub> in the upper troposphere and lower stratosphere, *Appl. Phys. Lett.*, **B75**, 183–194.
- Ridley, B., et al. (2004), Convective transport of reactive constituents to the tropical and mid-latitude tropopause region: I. Observations, *Atmos. Environ.*, **38**, doi:10.1016/j.atmosenv.2003.11.038, in press.
- Sassi, F., M. Salby, and W. G. Read (2001), Relationship between upper tropospheric humidity and deep convection, *J. Geophys. Res.*, **106**, 17,133–17,146.
- Schaffler, S. M., E. L. Atlas, D. R. Blake, F. Flocke, X. Tie, R. A. Lueb, J. M. Lee, V. Stroud, and W. Travnicek (1999), Distributions of brominated organic compounds in the troposphere and lower stratosphere, *J. Geophys. Res.*, **104**, 21,513–21,536.
- Schulte, P., and F. Arnold (1990), Pyridinium ions and pyridine in the free troposphere, *Geophys. Res. Lett.*, **17**, 1077–1080.
- Thompson, A. M., et al. (2003), Southern Hemisphere Additional Ozone-sondes (SHADOZ) 1998–2000 tropical ozone climatology: 1. Comparison with Total Ozone Mapping Spectrometer (TOMS) and ground-based measurements, *J. Geophys. Res.*, **108**(D2), 8238, doi:10.1029/2001JD000967.
- Tuck, A. F., et al. (1997), The Brewer-Dobson circulation in the light of high altitude in situ aircraft observations, *Q. J. R. Meteorol. Soc.*, **123**, 1–69.
- Tuck, A. F., S. J. Hovde, K. K. Kelly, M. J. Mahoney, M. H. Proffitt, E. C. Richard, and T. L. Thompson (2003), Exchange between the upper tropical troposphere and the lower stratosphere studied with aircraft observations, *J. Geophys. Res.*, **108**(D23), 4734, doi:10.1029/2003JD003399.
- Volk, C. M., et al. (1996), Quantifying transport between the tropical and mid-latitude lower stratosphere, *Science*, **272**, 1763–1768.
- E. L. Atlas, S. G. Donnelly, and V. R. Stroud, Atmospheric Chemistry Division, NCAR, Boulder, CO 80307, USA. (eatlas@rsmas.miami.edu; sdonnell@fhsu.edu; fridd@acd.ucar.edu)
- D. J. Cziczko, S. J. Hovde, K. K. Kelly, D. M. Murphy, E. A. Ray, S. J. Reid, E. C. Richard, D. S. Thomson, and A. F. Tuck, NOAA Aeronomy Laboratory, Boulder, CO 80305-3328, USA. (djciczko@al.noaa.gov; hovde@al.noaa.gov; kkelly@al.noaa.gov; murphyd@al.noaa.gov; eray@al.noaa.gov; sreid@nsf.gov; erik.c.richard@noaa.gov; atuck@al.noaa.gov)
- J. W. Elkins and F. L. Moore, NOAA Climate Monitoring and Diagnostics Laboratory, Boulder, CO 80305-3328, USA. (james.w.elkins@noaa.gov; fred.moore@noaa.gov)
- R. R. Friedl and M. J. Mahoney, Jet Propulsion Laboratory, California Institute of Technology, Pasadena, CA 91109, USA. (rfriedl@jpl.nasa.gov; michael.j.mahoney@jpl.nasa.gov)